PNAS RESEARCH ARTICLE | NEUROSCIENCE OPEN ACCESS

White matter plasticity following cataract surgery in congenitally blind patients

Caterina A. Pedersini[a,1], Nathaniel P. Miller[b,1], Tapan K. Gandhi[c,1], Sharon Gilad-Gutnick[d], Vidur Mahajan[e], Pawan Sinha[d], and Bas Rokers[a,f,2]

Edited by Thomas Albright, Salk Institute for Biological Studies, La Jolla, CA; received May 8, 2022; accepted February 25, 2023

The visual system develops abnormally when visual input is absent or degraded during a critical period early in life. Restoration of the visual input later in life is generally thought to have limited benefit because the visual system will lack sufficient plasticity to adapt to and utilize the information from the eyes. Recent evidence, however, shows that congenitally blind adolescents can recover both low-level and higher-level visual function following surgery. In this study, we assessed behavioral performance in both a visual acuity and a face perception task alongside longitudinal structural white matter changes in terms of fractional anisotropy (FA) and mean diffusivity (MD). We studied congenitally blind patients with dense bilateral cataracts, who received cataract surgery at different stages of adolescence. Our goal was to differentiate between age- and surgery-related changes in both behavioral performance and structural measures to identify neural correlates which might contribute to recovery of visual function. We observed surgery-related long-term increases of structural integrity of late-visual pathways connecting the occipital regions with ipsilateral fronto-parieto-temporal regions or homotopic contralateral areas. Comparison to a group of age-matched healthy participants indicated that these improvements went beyond the expected changes in FA and MD based on maturation alone. Finally, we found that the extent of behavioral improvement in face perception was mediated by changes in structural integrity in late visual pathways. Our results suggest that sufficient plasticity remains in adolescence to partially overcome abnormal visual development and help localize the sites of neural change underlying sight recovery.

dMRI | blindness | visual pathways | sight restoration | white matter plasticity

Significance

Our results shed light on white matter changes following treatment for congenital blindness late in childhood, after the closure of the sensitive period for visual development. We assessed whether sight recovery induced white matter plasticity and whether that plasticity was pathway specific and/or age dependent. We found that sight surgery induced considerable white matter plasticity in late-visual pathways. Due to the range of ages at which surgery occurred in our patients (from 7 to 17 y), we were able to establish that these experience-dependent changes were distinct from normal maturational changes. Overall, our results point to a sliding window of plasticity across the visual processing hierarchy and argue for a reevaluation of the conventional wisdom regarding sensitive period closure in visual development.

Congenital cataracts are a major cause of treatable blindness in children worldwide (1). While the prognosis for postoperative recovery of visual function is good in the developed world where surgery typically occurs in infancy (2), poor access to healthcare in the developing world means that many children grow up functionally blind (3–5). This difference in time in the access to treatment can cause a massive change in the recovery of visual skills in those patients. Thanks to seminal work (6), we know that there is a sensitive period early in life, during which the visual input is necessary for normal visual development as it molds structure and function of the visual brain network. In more recent studies, visual development has been described as characterized by multiple sensitive periods specific for different types of visual function [i.e., face perception (7)], during which the effects of visual experience on brain plasticity are particularly strong and lead to a full acquisition of normal function (8, 9). During sensitive periods, the development is characterized by rapid acquisition of stimulus-driven environmental statistics, while learning during adulthood is characterized by a larger top–down influence such as task relevance (for a review, see ref. 10).

The existence of sensitive periods during which brain reorganization is likely to be more pronounced has been confirmed by the cross-modal recruitment of the occipital cortex in response to tactile or auditory stimuli not only in early-blind individuals, but also in late-blind individuals (8, 11–14). This cross-modal plasticity can be explained following either the metamodal conception of the brain (15) as composed of cortical regions that have intrinsic functional roles but flexible modality preferences or the pluripotent conception of the brain (16) as composed of cortical areas capable of assuming a heterogeneous range of functional roles.

The existence of sensitive periods in the development of visual function would suggest that providing surgical care for congenital cataracts in adolescence will have limited impact after the sensitive period for visual development has closed around 5 to 7 y of age (17), although the exact timing will change depending on the particular visual function under consideration. However, recent work on the clinical population under consideration here has shown that surgery, even when provided in late childhood, can lead to major improvements in perceptual abilities (18–20). Perceptual gains include

Author contributions: P.S. and T.K.G designed research; T.K.G. performed research; C.A.P., N.P.M., and B.R. analyzed data; C.A.P., N.P.M., and B.R. methodology; T.K.G. data collection shared first authorship; S.G.-G. and V.M. data collection; C.A.P., N.P.M., T.K.G., S.G.-G., V.M., P.S., and B.R. wrote the paper.

The authors declare no competing interest.

This article is a PNAS Direct Submission.

[1]C.A.P., N.P.M., and T.K.G. contributed equally to this work.

[2]To whom correspondence may be addressed. Email: rokers@nyu.edu.

This article contains supporting information online at https://www.pnas.org/lookup/suppl/doi:10.1073/pnas.2207025120/-/DCSupplemental.

Published May 1, 2023.

improvements in low-level perceptual measures such as visual acuity and contrast sensitivity as well as in higher-level visual function such as face perception. As described by refs. 21 and 22, different behavioral studies on multiple clinical populations show considerable individual variability in the amount of visual acuity improvement after cataract surgery.

These perceptual gains can be characterized as visual perceptual learning, defined as the improvement in visual task performance with practice or training (23). Perceptual learning produces gains in visual performance in patients affected by cortical blindness (24). The activation of spared regions of V1 (25) or the reorganization of subcortical pathways (26) can explain the improvement of performance in visual tasks as a consequence of extensive visual training. This residual developmental neuroplasticity retained by the adult brain even after the closure of the sensitive periods can explain the perceptual gains reported in blind individuals after sight restoration (27–30).

Amblyopia is a neurodevelopmental visual disorder that arises from abnormal visual experience (e.g., degraded or misaligned visual image to one eye) during sensitive periods (31). Prior work on this typical model of abnormal visual development suggests that alternative networks of neural areas are recruited to support visual perception by the amblyopic eye in the case of stereopsis (32, 33) and motion integration (32, 33). The recruitment of a different neural network is an example of residual neuroplasticity of the amblyopic brain, even after the closure of a sensitive developmental period.

Neuroplasticity in the adult healthy brain has been assessed by asking normally sighted observers to learn a complex visuomotor task such as juggling (34) or to acquire expertise with novel classes of visual objects (35). These results suggest that parts of the visual system remain plastic even after the early sensitive period. While the early visual cortex shows little change in these studies, extrastriate visual areas exhibit structural and functional changes as new skills are acquired. However, these studies rely on healthy adults in whom early-visual pathways have developed normally, leading to typical visual input to extrastriate areas. To overcome this limitation, research on nonhuman primates (36) as well as multiple electrophysiological and neuroimaging studies on humans explored the different degree of recovery of the primary visual cortex (V1) as opposed to extrastriate visual areas in sight recovery subjects (37, 38). In summary, they observed that visual areas that develop later and more slowly are more affected by a lack of visual stimulation at birth than visual areas that mature earlier and faster. That explained the higher dependence on visual experience of cortical development in extrastriate than striate regions (39–41).

In this study, we investigated the potential for long-term white matter change in patients with congenital cataracts who acquire patterned retinal input after removal of the lenticular opacity and implantation of an artificial lens during adolescence. We assessed behavioral performance in both visual acuity and face discrimination tasks and compared diffusion-derived white matter properties at multiple postoperative timepoints to preoperative baselines in major white matter pathways of the human brain. Since the age at intervention varied across patients, we were able to determine the extent to which plasticity depended on the age at onset of patterned vision. Additionally, we include healthy age-matched normative data from the Human Connectome Project–Developmental (HPCD) dataset (42) to evaluate the impact of congenital blindness as well as cataract surgery on white matter properties. Given the observed improvements in perceptual performance in patients treated late for congenital blindness, we hypothesized that the restored visual input improves behavioral performance in both low- and higher-level visual function and can lead to long-term change in the structural properties of local circuits in later stages of the visual hierarchy, even after closure of the putative sensitive period.

Results

Assessing the Behavioral Impact of Cataract Surgery. We longitudinally followed 19 cataract patients (6 female), aged 7 to 16 y (mean age of 11.22 ± 2.85 y at the time of surgery) and tracked behavioral measures during adolescence. The longitudinal effects of time since surgery and age at measurement on visual acuity performance were assessed using a linear mixed-effects (LMEs) model (see the *Methods* section for details). Visual acuity (Fig. 1 *A* and *B*) significantly improved following cataract surgery ($F(1,142) = 6.45$, $P = 0.012$). As in a previous report with either a larger (18) or a smaller cohort (19, 20), we found no relationship between visual acuity and patient age at measurement ($F(1,142) = 0.28$, $P > 0.05$). This result is not surprising when considering the existence of a sensitive period in the development of visual acuity. Moreover, visual acuity did not depend on the interaction between time since surgery and patient age at behavioral measurement ($F(1,142) \cong 0$, $P > 0.05$) (Fig. 1*E*).

The majority of improvement in visual acuity occurs in the first few days after surgery and is best captured by a model expressing the change in visual acuity as a function of log-transformed time since surgery [BIC (Bayesian information criterion) = 33.91] than linear time since surgery (BIC = 66.86). We note that although we saw substantial improvements in acuity, with many patients having no pattern vision prior to surgery, few patients achieved acuity greater than 20/200 at any time after surgery. The majority of patients therefore remain classified as legally blind after surgery (18–20), even though these modest perceptual improvements lead to major benefits in quality of life for these patients (43).

Visual acuity is a measure of perceptual function that depends on the integrity of early parts of the visual system. To behaviorally assess the integrity of later parts of the visual system, patients were asked to perform a task in which they discriminated pictures of faces from other nonface stimuli (see ref. (20) for details). Preoperatively, the majority of patients performed near chance in this task (d' ~ 0, Fig. 1 *C* and *D*). Using the same LMEs model applied to the visual acuity data above, we found that face discrimination also significantly improved following cataract surgery ($F(1, 75) = 30.91$, $P < 0.001$). Similar to visual acuity, the majority of improvement occurred shortly after surgery (Fig. 1*D*; log-transformed model BIC:230.89, linear model BIC: 275.87). We found no relationship between face discrimination and patient age at measurement ($F(1, 75) = 1.06$, $P > 0.05$). However, we did find a significant interaction between patient age and time since surgery ($F(1, 75) = 5.61$, $P = 0.02$). Inspection of the model coefficients reveals that surgery-related change in performance was greater for patients who received surgery at a younger age. We found similar results when excluding those patients who performed above chance before surgery (P07/P08/P20). Indeed, in this case, we found a significant effect of surgery ($F(1, 61) = 31.803$; $P < 0.01$) and a significant interaction between surgery and age at measurement ($F(1, 61) = 5.837$; $P = 0.018$), while the effect of age was not significant ($F(1, 61) = 0.8$; $P = 0.37$). Also in this case, BICs revealed that log-transformed time since surgery provided a better prediction of the observed data (log-transformed model BIC:188.85, linear model BIC: 224.56).

To visualize the nature of this interaction, we derived the change in face discrimination performance over time since surgery for each patient using the polynomial curve fitting matlab function

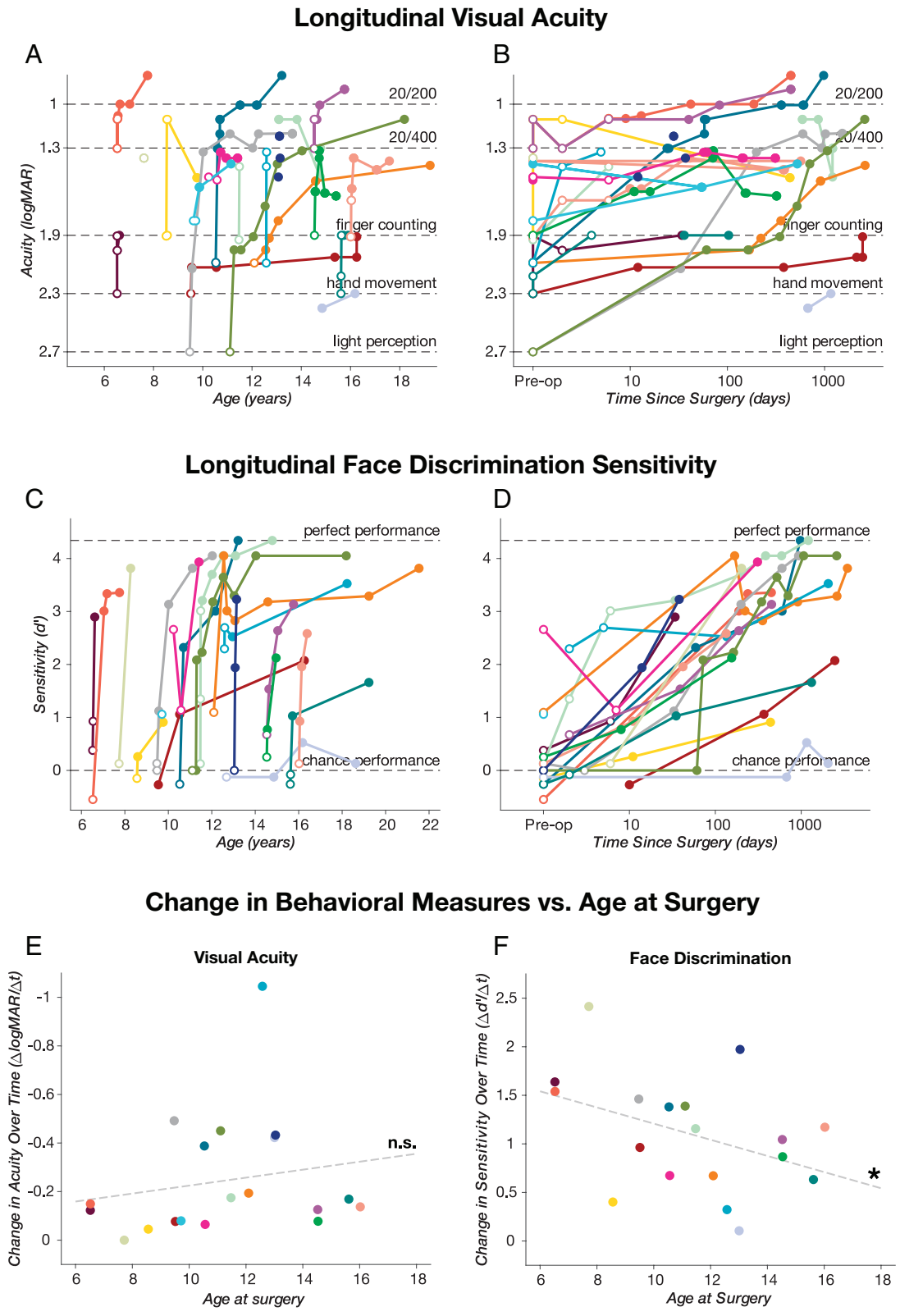

Fig. 1. Summary of longitudinal performance in visual acuity and face discrimination tasks. Longitudinal logMAR visual acuities and face vs. nonface discrimination (reported as d-prime), plotted against age at the time of measurement (*A* and *C*) and time since surgery on a logarithmic scale (*B* and *D*). Closed points mark performance recorded more than 1 wk after surgery; open points mark performance recorded preoperatively and up to 7 d postoperatively. For all panels, each color represents a single subject, with longitudinal time points connected by solid lines in panels *A*–*D*. In panels *A* and *B*, dashed lines indicate levels of relative visual acuity (from bottom to top; light perception, hand movement, finger counting, 20/400, and 20/200). In panels *C* and *D*, dashed lines indicate relative task performance (bottom line, chance performance; top line, maximum performance). Panels *E* and *F* display derived rates of behavioral change over time since surgery (delta d′/delta t) plotted against age at the time of surgery [(*E*) visual acuity data; (*F*) face perception data]. Dashed gray lines present the least-squares regression fit to the data. * indicates a statistically significant interaction in the linear mixed-effect model (age at measurement * time since surgery; $P < 0.05$).

(polyfit). We obtained one value of change over time for each patient. Then, we plotted the derived data as a function of age at surgery (Fig. 1*F*). The significance of this effect is derived from the interaction effect of the model, taking into account the estimates of each predictor in isolation. These results suggest that, while there is no evidence that time of surgery affects the visual acuity improvement for these patients, face discrimination depends on a closing window of neural plasticity whereby surgery at a later age reduces the behavioral improvement.

Evaluating White Matter Properties. To examine the link between behavioral improvements in visual perception and underlying neuroanatomical change, we examined white matter plasticity in ten major pathways that span the visual processing hierarchy. We categorized these white matter tracts into early-visual, late-visual, and non-visual pathways for the purposes of this study. Early-visual pathways included the optic radiation (OR) and the optic tract (OT). Late-visual pathways included the inferior fronto-occipital fasciculus (IFOF), the superior longitudinal fasciculus (SLF), the inferior longitudinal fasciculus (ILF), and the posterior callosum forceps. The non-visual pathways included the cingulate cingulum (CC), the cortico-spinal tract, the uncinate fasciculus, and the anterior callosum forceps.

Fig. 2 illustrates tract profiles, as well as their change over time, for one representative patient (P02). In supplementary material, we show the mean and SE of tract profiles of patients and controls (see *Methods* for a complete explanation of the procedure) (*SI Appendix*, Fig. S2).

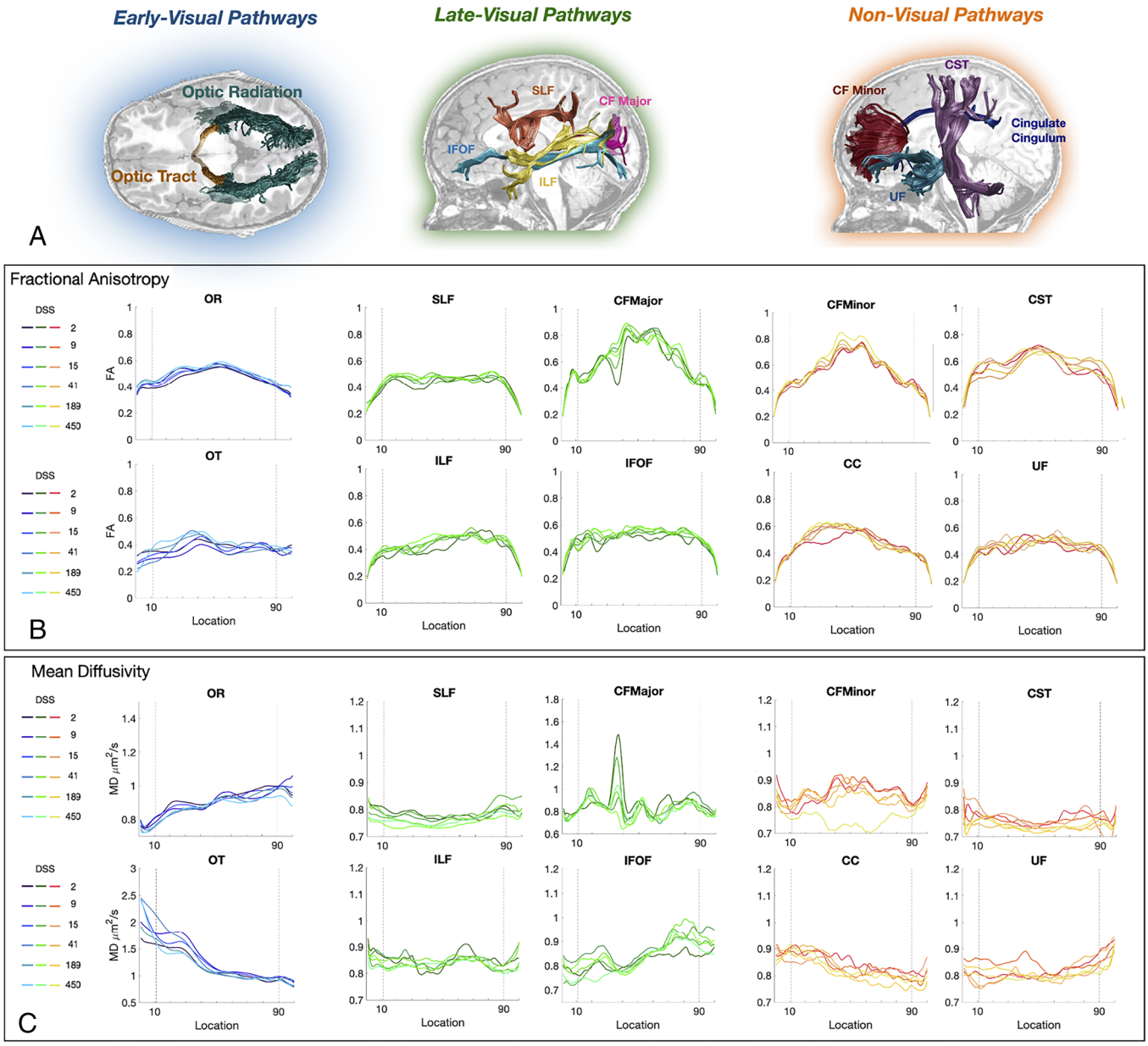

Fig. 2. Patient white matter tract profiles—fractional anisotropy (FA) and mean diffusivity (MD) values. Tractography-generated white matter pathways are grouped according to early-visual, late-visual, and non-visual pathways. (*A*) Illustration of the white matter pathways overlaid on a structural T1 slice in a representative cataract patient (P02). Early-visual pathways: optic tract (OT) and optic radiation (OR). Late-visual pathways: posterior callosum forceps (CFMajor), superior longitudinal fasciculus (SLF), inferior fronto-occipital fasciculus (IFOF), and inferior longitudinal fasciculus (ILF). Non-visual pathways: corticospinal tract (CST), cingulum cingulate (CC), anterior callosum forceps (CFMinor), and uncinate fasciculus (UF). For late- and non-visual pathways, only left hemisphere pathways are shown. (*B* and *C*), Plots of FA/MD values as a function of location along the tract at multiple points of assessment [days since surgery (DSS) post-intervention; see legend] in a representative patient (P02). FA and MD values are plotted from anterior (*Left*) to posterior (*Right*).

Identifying White Matter Change due to Typical Maturation. In typical development, pathway density, organization, and myelination change, and is reflected in decreased mean diffusivity (MD) and increased fractional anisotropy (FA) (44–47). Thus, our work here introduces a unique challenge because it involves identifying white matter changes due specifically to sight restoration above and beyond these typical maturational changes. We estimated maturational structural change in our dataset in terms of FA and MD measures in two ways. First, we considered patients as controls of each other, taking into account the wide age range included in our patient database, the range of ages at surgery and the longitudinal collection of data. Advantages of this patients-only method are the control of environmental and socioeconomic factors within the patient population and reliance on the same protocol sequence used to acquire data. Nevertheless, a possible confound in this case is the "sleeper effect," the fact that visual deprivation during a specific period previous to either the first manifestations of a functional ability (e.g., face perception) or the development of structural measures can affect its later development (48). To control for this potential confound, we also conducted controls-included analyses that included a group of 80 age-matched controls in the analysis, which reflect the typical development of structural measures in a healthy population. For both methods of analysis (*Methods*), we found a medium or strong correlation ($r > 0.38$; $r > 0.39$) between empirical and predicted structural measures for each tract using a cross-validated leave-one-out method.

In this section, we describe the age-related maturation effects in our measures of white matter pathway integrity. In the patients-only analysis, we identified significant maturation effects in two late-visual pathways: the posterior callosum forceps ($F(1, 46) = 6.7232$, P-value = 0.013, false discovery rate (FDR) = 0.0477) and the ILF ($F(1, 46) = 11.217$, P-value = 0.0016, FDR = 0.0477) (*SI Appendix*, Table S1). In both tracts, the beta estimates of the fixed effect were positive, showing an increase of FA as a function of age.

In the controls-included analysis, we found significant changes in MD related to typical maturation in all non-visual as well as in three late-visual pathways (posterior callosum forceps, ILF, and SLF). All the estimates of the age-related effect were negative, indicating a decrease in MD with increasing age, and so an increase of white matter integrity as a function of age. Regarding FA, we found significant results mainly in late-visual pathways (posterior callosum forceps, ILF, SLF, and IFOF), in one non-visual pathway (CC) and in the OR. All the estimates in this case were positive, indicating an increase of pathway integrity with increasing age, as expected during adolescence (49, 50). When considering healthy controls, we observed that the expected age-related development of diffusion measures is represented by a decrease of MD and an increase of FA as a function of age. The same trend can be observed in all patients.

Maturational trends for selected pathways are shown in Figs. 3–5 (top row). In each figure, the dashed red line represents the best linear fit for the full model, such that the slope illustrates the fixed effect of age at measurement in our sample (patients and controls). We also plotted the observed and predicted values with their CI for each subject, structural measure, and Diffusion Tensor Imaging (DTI) session in *SI Appendix*, Fig. S4 to help visualize the goodness-of-fit of our model.

Thus, merging together the MD and FA results, we observe a significant maturational effect on all white matter pathways, except for the OT where the trend followed the expected direction (decrease of MD and increase of FA as a function of age), but the magnitude of the changes might have been too small or variable to reach significance. This effect reflects typical maturational changes in structural measures. Regardless of significance, we incorporated the estimated effects of age on white matter properties in all subsequent analyses. A full summary of age-related effects on white matter structure is provided in *SI Appendix*, Tables S2–S4.

Identifying White Matter Change Following Sight Recovery.

Absence of plasticity in early-visual pathways. When measuring white matter change in early-visual pathways using the patient-only analysis, we did not find any significant effect but only a general trend of structural integrity increasing as a function of time since surgery [FA OT $F(1, 46) = 5.56$, P-value = 0.02, FDR = 0.067; FA OR $F(1, 46) = 3.2464$, P-value = 0.078, FDR = 0.13; MD OT $F(1, 46) = 2.94$, P-value = 0.09, FDR = 0.28; MD OR $F(1, 46) = 1.04$, P-value = 0.31, FDR = 0.49]. In the controls-included analysis, we found only a marginal significant relationship between sight-recovering treatment and structural plasticity in the OT, as measured by FA ($F(1, 125) = 5.49$, P-value = 0.021, FDR = 0.051). This trend indicates an increase of FA as a function of time since surgery. This result is affected by the specific value assigned to controls, as it disappears when assigning a different value to the time since surgery of controls (value of 0; see *SI Appendix*, Table S2 and a description in the *SI Appendix*, *Methods* section). Moreover, the distribution of P-values shown in *SI Appendix*, Fig. S5 clearly indicates that the percentage of significant P-values is low (17.56%). In addition, results are far from significant in the OR, when considering both FA and MD [FA $F(1, 125) = 2.87$, P-value = 0.09, FDR = 0.14; MD $F(1, 125) = 0.16$, P-value = 0.69, FDR = 0.81].

Overall, the absence of surgery-related effects in these early visual pathways is consistent with the notion that the sensitive period for development of the early-visual system has closed, with little evidence for reopening of the critical window despite the onset of visual input. This result is confirmed by the significant difference (uncorrected p-values) between groups in early-visual pathways: The structural integrity of controls is greater than in patients, indicating that the development of these tracts depends in part on visual experience (*SI Appendix*, Tables S3 and S4). This trend was the same when including all and reduced volumes of controls, with bigger between-group differences when including all volumes (*SI Appendix*, Fig. S3). Results are shown in Fig. 3, *Bottom Row*.

Plasticity in late-visual pathways. In contrast to early visual pathways, we found significant surgery-related effects in late-visual pathways in both patients-only and controls-included analyses. Specifically, treatment was associated with white matter structural change, as measured by FA, in three of the four pathways: the SLF [patients-only: $F(1, 45) = 6.8164$, P-value = 0.012, FDR = 0.0477; controls-included: $F(1, 124) = 6.8288$, P-value = 0.01, FDR = 0.031], the ILF [patients-only: $F(1, 46) = 7.0342$, P-value = 0.011, FDR = 0.0477; controls-included: $F(1, 124) = 7.65$, P-value = 0.007, FDR = 0.0262], and the IFOF [patients-only: $F(1, 45) = 6.9025$, P-value = 0.012, FDR = 0.0477; controls-included: $F(1, 124) = 6.579$, P-value = 0.012, FDR = 0.0329].

In addition, treatment was associated with white matter structural change, as measured by MD, in the posterior callosum forceps [patients-only: $F(1, 44) = 17.677$, P-value < 0.001, FDR = 0.0038; controls-included: $F(1, 122) = 14.763$, P-value < 0.001, FDR < 0.001]. The estimates of these tracts highlight an increase of structural integrity (higher FA and lower MD) as a function of time since surgery, indicating that the visual stimulus onset is associated with an increase of structural integrity in interhemispheric and intrahemispheric white matter pathways that connect the occipital cortex with the ipsilateral frontal, parietal, and temporal cortex as well as with contralateral occipital regions. Results are shown in Fig. 4, *Bottom Row*. To show that these results do not

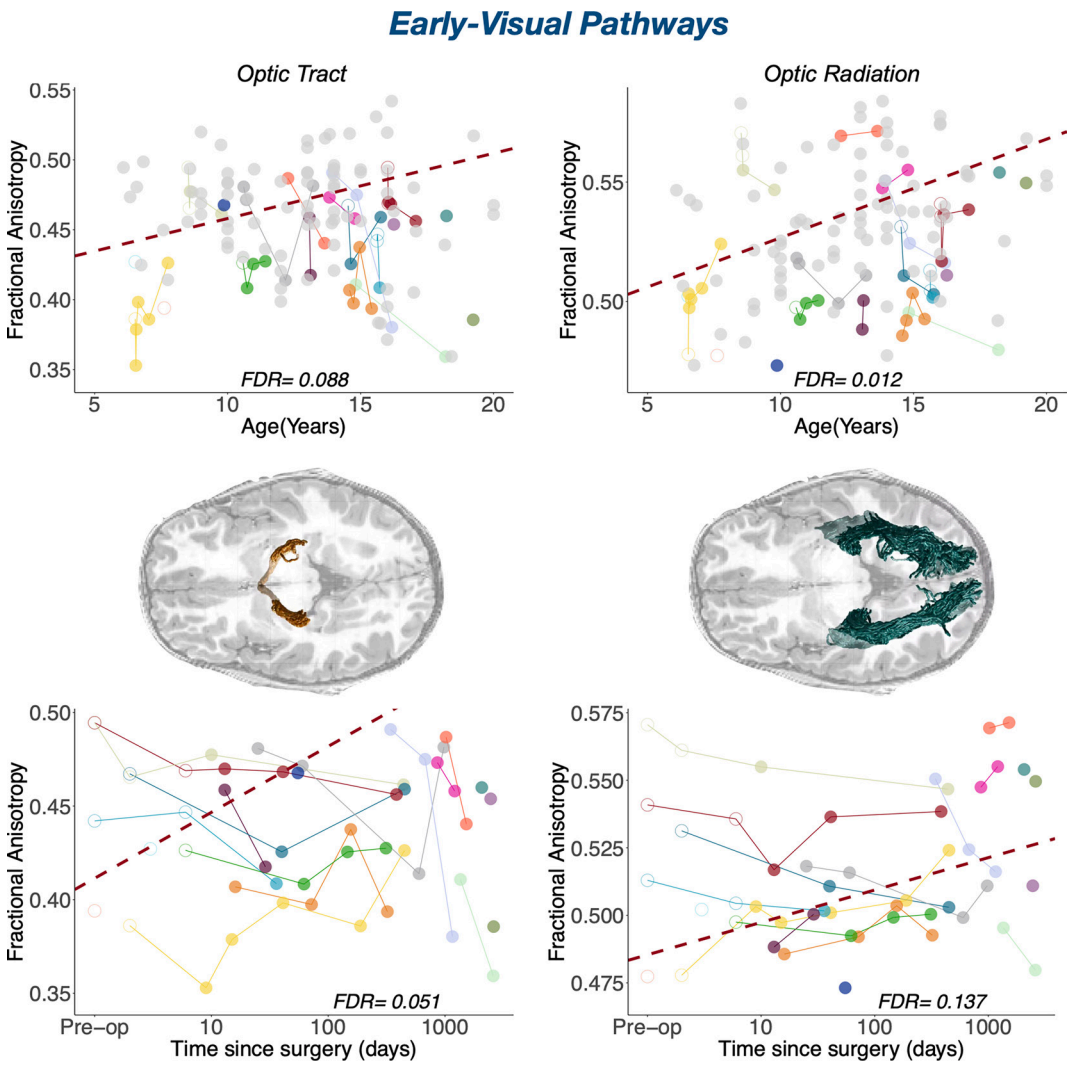

Fig. 3. Maturational and longitudinal changes in early-visual white matter pathways. Maturational and longitudinal changes in fractional anisotropy for optic tract and optic radiation are plotted as a function of age at measurement (*Top Row*) and time since surgery (*Bottom Row*). Each color represents a single patient, with longitudinal time points connected by solid lines. Closed points mark DTI sessions acquired more than 1 wk after surgery; open points mark DTI sessions acquired as maximum 7 d after surgery. Dots color-coded in light gray in the left plots represent controls. The dashed red line represents the best linear fit for the LME model, such that the slope represents the beta of the fixed effects (age at measurement on the *Top Row* and time since surgery on the *Bottom Row*) and the intercept represents the group intercept of the random effect. FDR values represent the corrected p-values of the specific fixed effect (age on the *Top Row*; time since surgery on the *Bottom Row*) extracted from the LME model: *Pathway MD/FA ~ Group + Log DaysSinceSurgery * Age at Measurement + (1|Subject).* In the central row, we represent the specific white matter pathway that the results on the same row correspond to overlaid on an axial T1 slice in a representative cataract patient (P02).

depend on the specific values assigned to the time since surgery of controls, we check the distribution of *P*-values after assigning random values to the time since surgery of controls, as described in the *Method* section.

The results in *SI Appendix*, Fig. S5 show that for late-visual pathways, the distribution of *P*-values is skewed toward zero, indicating a higher probability of significant results when assigning random values to the time since surgery of controls. These uncorrected p-values are significant also when assigning zero to the time since surgery of controls but do not survive the FDR correction for multiple comparison in ILF and SLF.

Limited plasticity in non-visual pathways. When measuring white matter change in non-visual pathways applying the patients-only analysis, we did not find any significant effect of the treatment after correcting for multiple comparisons (*SI Appendix*, Table S1).

When we apply the controls-included analysis, we observed a significant effect of time since surgery only in the MD of the anterior callosum forceps (F(1, 125) = 9.7176, *P*-value = 0.002, FDR = 0.0057), connecting the lateral and medial surfaces of frontal lobes. The results did not change when we assigned a value of 0 to the logarithmic scale of time since surgery of patients (*SI Appendix*, Table S2). When considering the histograms of *P*-values distributions, we see that this non-visual pathway shows a distribution of p-values skewed toward zero, confirming the significance of the fixed effect (*SI Appendix*, Fig. S5). A full summary of surgery-related effects on white matter structure is provided in *SI Appendix*, Tables S2–S4. Results are shown in Fig. 5, *Bottom Row*.

Overall, our results show that the structural integrity of late-visual pathways that connect the occipital cortex with ipsilateral frontal/temporal/parietal regions or with homotopic regions in the contralateral hemisphere is significantly affected by cataract surgery with great improvement after visual restoration received even after the putative closure of the sensitive period.

Impact of Age at Treatment on White Matter Plasticity. We next asked whether the potential for white matter plasticity may depend on the patient's age at the time of treatment.

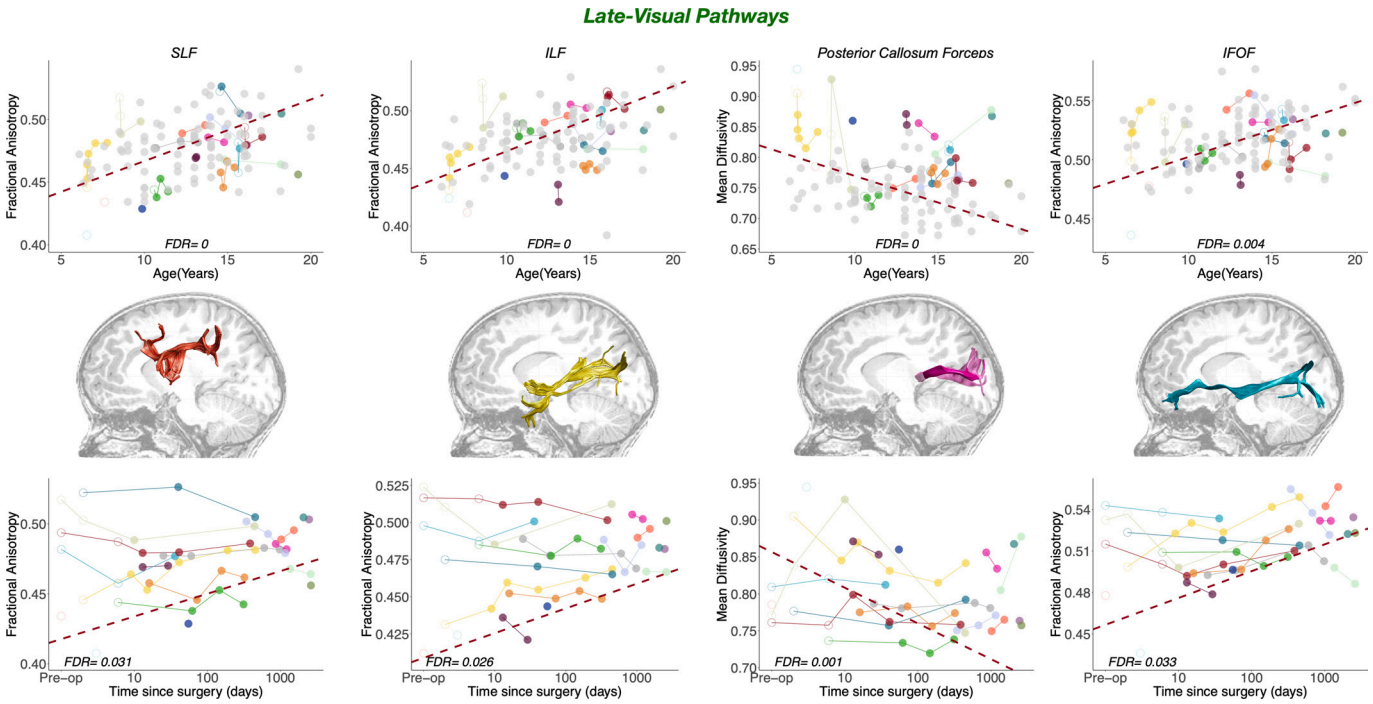

Fig. 4. Maturational and longitudinal changes in late-visual white matter pathways. Maturational and longitudinal changes in fractional anisotropy for late-visual pathways are plotted as a function of age at measurement (*Top Row*) and time since surgery (*Bottom Row*). Each color represents a single patient, with longitudinal time points connected by solid lines. Closed points mark DTI sessions acquired more than 1 wk after surgery; open points mark DTI sessions acquired as maximum 7 d after surgery. Dots color-coded in light gray in the left plots represent controls. The dashed red line represents the best linear fit for the LME model, such that the slope represents the beta of the fixed effects (age at measurement on the *Top Row* and time since surgery on the *Bottom Row*), and the intercept represents the group intercept of the random effect. FDR values represent the corrected *P*-values of the specific fixed effect (age on the *Top Row*; time since surgery on the *Bottom Row*) extracted from the LME model: *Pathway MD/FA ~ Group + Log DaysSinceSurgery * Age at Measurement + (1 | Subject).* In the central row, we represent the white matter pathway that the results on the same row correspond to, overlaid on a sagittal T1 slice in a representative cataract patient (P02). SLF, superior longitudinal fasciculus; ILF, inferior longitudinal fasciculus; IFOF, inferior fronto-occipital fasciculus.

Such findings would support reductions in plasticity during adolescence across the visual processing hierarchy. We found such a relationship based on the interaction between age at treatment and time since surgery in both patients-only and controls-included analysis (see Fig. 6 for the results of the second family or controls-included LME models). In early-visual pathways, we found evidence for such an interaction in the OT for FA [patients-only: $F(1, 46) = 7.69$, P-value = 0.008, FDR = 0.0477; controls-included: $F(1, 125) = 7.07$, P-value = 0.009, FDR = 0.0303]. In late-visual pathways, we found evidence in the ILF [patients-only: $F(1, 46) = 8.97$, P-value = 0.004, FDR = 0.0477; controls-included: $F(1, 124) = 9.29$, P-value = 0.003, FDR = 0.014] and SLF [patients-only: $F(1, 45) = 7.48$, P-value = 0.009, FDR = 0.0447; controls-included: $F(1, 124) = 7.87$, P-value = 0.006, FDR = 0.026] for FA and in the posterior callosum forceps for MD [patients-only: $F(1, 44) = 12.1$, P-value = 0.001, FDR = 0.0172; controls-included: $F(1, 125) = 4.03$, P-value = 0.04, FDR = 0.014]. The negative estimates of the predictors in the case of FA and the positive estimates in the case of MD indicate that in these tracts, we observe higher tract integrity after surgery depending on the age of patients: Young patients show greater impact of treatment than older patients. These significant effects indicate that interventions early in adolescence, but past the traditional sensitive period, resulted in greater structural change than interventions later in adolescence.

Identifying the Effects of Surgery on Behavior Mediated by White Matter Change. An important and still unanswered question is whether the patient's behavioral visual improvements following surgical intervention can be attributed more directly to structural changes in any specific white matter pathway. To answer this, we conducted a mediation analysis that determined whether the observed white matter change in any particular pathway predicted the behavioral improvement and reduced the indirect relationship between surgery and perceptual improvement when evaluated concurrently. We first linearly interpolated acuity and face perception measures to the day(s) of diffusion MRI (dMRI) measurement given that behavioral and dMRI measurements were not always collected on the same day. We used the *interp1* matlab function to assign missing behavioral measures to diffusion timepoints based on the empirical data. We did not evaluate dMRI measurements in cases where no behavioral measurements straddled the dMRI data, so our analysis necessarily includes only a subset of all behavioral and dMRI data collected and reported above (P08/19 were excluded from visual acuity; P08/09/19/21 were excluded from face perception).

Then, we assessed the relationship between treatment, structural measures, and interpolated behavioral performance by models that included the specific predictor, the fixed effect of age at measurement and their interaction. Significant results would highlight the presence of a predictive effect of surgery over outcome, surgery over structural measure changes, or structural changes over behavioral outcome, while controlling for age. In this way, we could select a subsample of tracts that showed a significant effect in all these pairwise relations.

Time since surgery directly predicted interpolated performance in the face discrimination task (beta = 1.71, $F(1, 34) = 32.835$, $P < 0.001$), while the result was not significant when considering the interpolated performance in the visual acuity task (beta = −0.15, $F(1, 42) = 1.67$, $P = 0.203$). The relationship between surgery and

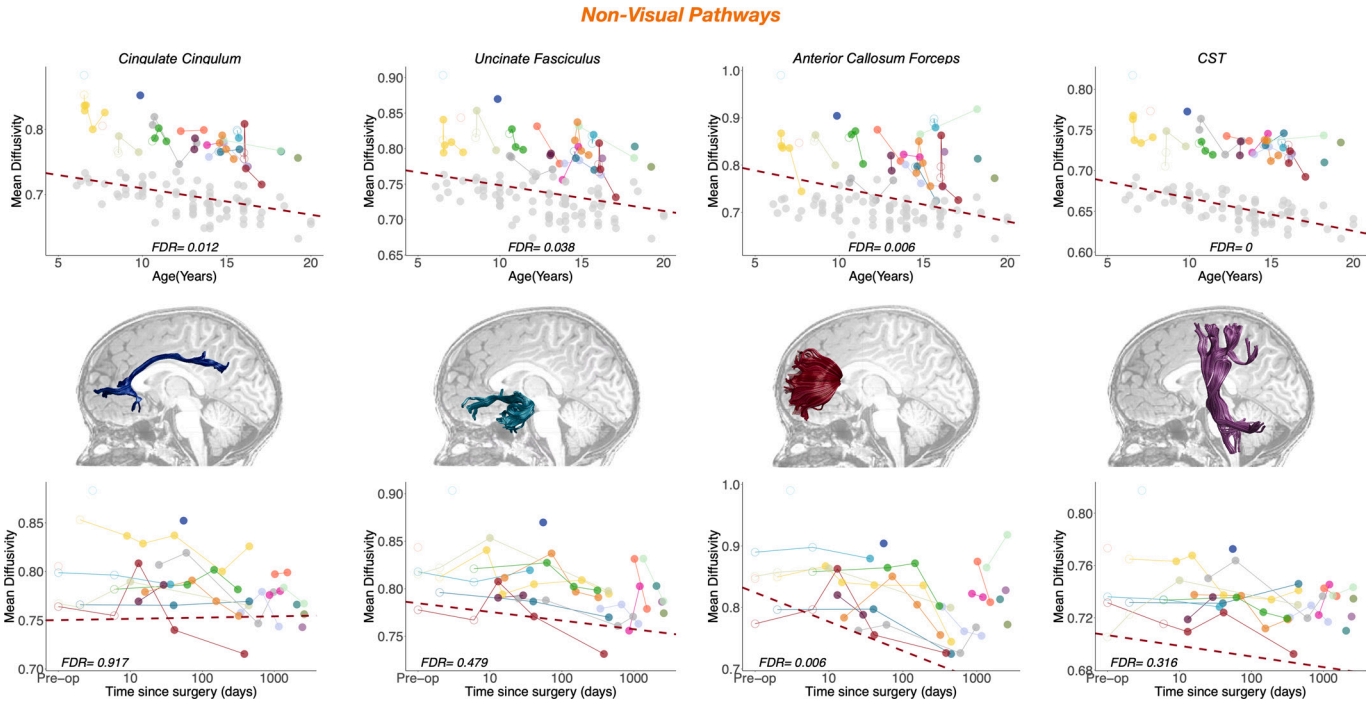

Fig. 5. Maturational and longitudinal changes in non-visual white matter pathways. Maturational and longitudinal changes in fractional anisotropy for non-visual pathways are plotted as a function of age (*Top Row*) and time since surgery (*Bottom Row*). Each color represents a single patient, with longitudinal time points connected by solid lines. Closed points mark DTI sessions acquired more than 1 wk after surgery; open points mark DTI sessions acquired as maximum 7 d after surgery. Dots color-coded in light gray in the left plots represent controls. The dashed red line represents the best linear fit for the LME model, such that the slope represents the beta of the fixed effects (age at measurement on the *Top Row* and time since surgery on the *Bottom Row*), and the intercept represents the group intercept of the random effect. FDR values represent the corrected p-values of the specific fixed effect (age on the *Top Row*; time since surgery on the *Bottom Row*) extracted from the LME model: *Pathway MD/FA ~ Group + Log DaysSinceSurgery * Age at Measurement + (1 | Subject).* In the central row, we represent the specific white matter pathway that the results on the same row correspond to, overlaid on a sagittal T1 slice in a representative cataract patient (P02). CST, cortico-spinal tract.

structural measures was previously assessed and resulted in an increase of structural integrity as a function of surgery in late-visual pathways, indicating that surgery predicted structural changes in those tracts. Finally, we selected those tracts that predict the interpolated d-prime: the posterior callosum forceps [MD - beta = −43.104, $F(1, 32) = 6.46$, $P = 0.016$], IFOF [FA - beta = 114.99, $F(1, 33) = 12.02$, $P = 0.0015$], and SLF [FA - beta = 85.593, $F(1, 33) = 5.3271$, $P = 0.027$].

On this subsample of late-visual tracts, we performed mediation analysis using a three-variable path model (51, 52). When conducting the mediation analysis without controlling for the interaction effect, we did not observe any significant mediation effect but only significant connections between two of the three variables included in the model. Instead, when controlling for the interaction between predictor and mediator, we observed a significant modulation of the association between surgery and behavioral outcome by means of structural changes in the posterior callosum forceps (Fig. 7). The significant interaction effect, in addition to the absence of a significant fixed effect of the mediator, confirms that the MD of the posterior callosum forceps is acting

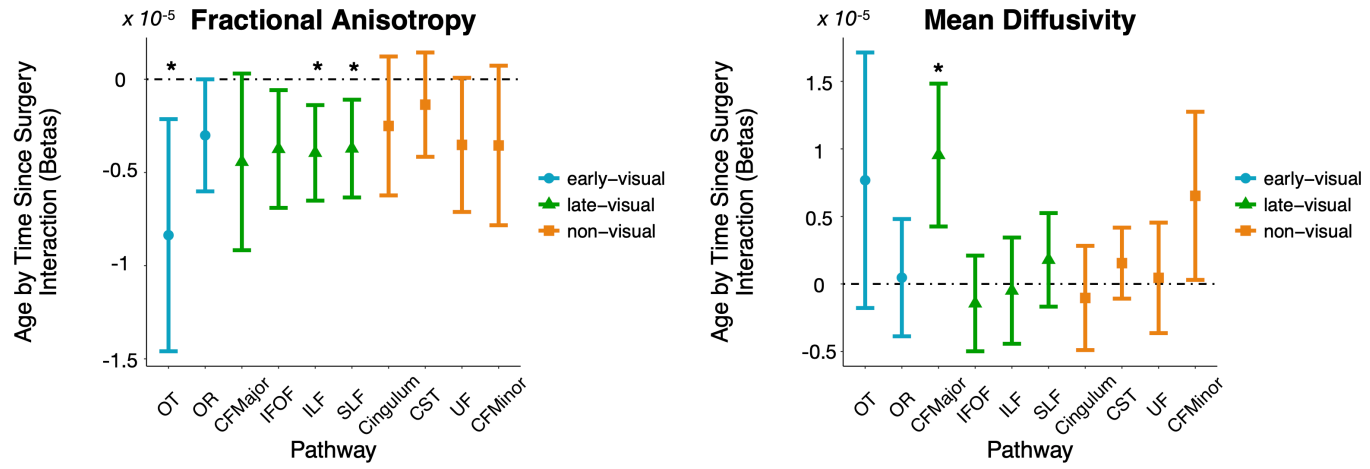

Fig. 6. White matter plasticity varies with age at measurement. Age at measurement by time since surgery interaction effects (beta weights) plotted for early-visual (blue), late-visual (green), and non-visual (orange) pathways for fractional anisotropy (*Left*) and mean diffusivity (*Right*). Pathways for which the interaction effect passes multiple-comparisons correction (FDR < 0.05) are marked by *****. OT, optic tract; OR, optic radiation; CFMajor, posterior callosum forceps; IFOF, inferior fronto-occipital fasciculus; ILF, inferior longitudinal fasciculus; SLF, superior longitudinal fasciculus; CST, cortico-spinal tract; UF, uncinate fasciculus; CFMinor, anterior callosum forceps.

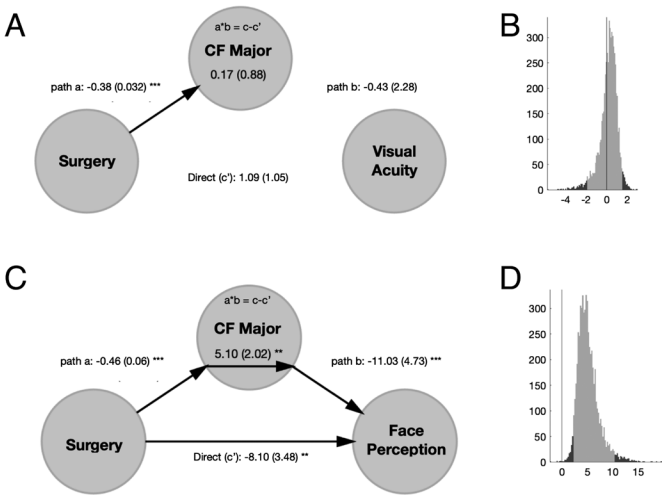

Fig. 7. Mediation analysis for visual acuity and face perception. Results of the mediation analysis testing the relationship among surgery, mean diffusivity of the posterior callosum forceps, and interpolated dprime in the face discrimination task or interpolated logMAR for the visual acuity task after controlling for the interaction effect. (*A*–*C*). Model with the path coefficients (*A* for visual acuity; *B* for face perception) and the SEM in parentheses, significant at $*P = 0.01$, $**P = 0.005$, $**P = 0.001$. (*B*–*D*). Histogram of the bootstrapped distribution (1,000 repetitions) of the mediation effect (a*b = c– c) for visual acuity (*B*) and face perception (*D*). The lighter gray portion of the histogram denotes the 95% CI for the effect.

as a moderator of the association between surgery and interpolated behavioral outcome. The positive coefficient linking surgery to d-prime, passing through structural changes, indicates that the effect of treatment over outcome is positive (surgery leads to better performance) and can be explained in part by the changes in structural integrity. As a confirmation of the modulatory effect, time since surgery still impacted behavioral face discrimination performance even after accounting for the white matter properties (direct path c' still significant).

Overall, our results indicate that cataract surgery in adolescence leads to changes in white matter properties as well as improvements in visual face perception. Importantly, some of the perceptual improvements in face perception, but not acuity, are directly modulated by plasticity in white matter increase of structural integrity of the posterior callosum forceps which connect the bilateral occipital regions.

Discussion

In this study, we assessed behavioral and structural white matter changes following late sight recovery in congenitally blind patients. Patients experienced significant improvements in low-level vision. Indeed, logMAR (logarithmic of the minimum angle of resolution) visual acuity improved significantly postoperatively. These results are in agreement with previous studies that showed a rapid improvement of visual acuity and contrast sensitivity after visual restoration, even when the treatment was received later in life (19, 53, 54). This effect was specific to surgery, as neither an isolated effect of age nor an interaction between age and time since surgery was found. However, we did not find evidence that the improvements in visual acuity were linked to changes in specific white matter pathways.

Patients also demonstrated significant improvement in a behavioral face discrimination task following surgery. The recovery of face recognition skills in congenitally blind individuals after visual restoration has been reported in previous studies on the same (20) and on different clinical populations (55). In contrast to the visual acuity results, we identified a significant interaction between patient age and time since surgery, with patients who received surgery at a younger age experiencing larger improvement in this task. This interaction is consistent with a sliding window of plasticity for learning higher-order visual tasks, wherein patients who receive intervention earlier achieve better outcomes. Finally, we linked these behavioral improvements to specific neuroanatomical changes following surgical intervention.

The main neuroimaging findings of this study are represented by the surgery-related changes in some white matter pathways, even after controlling for the maturational effects. The increase of FA and decrease of MD observed in this study after visual restoration due to treatment have been suggested to reflect increased myelination, growth of axon caliber, and reduced free extracellular water (56) that can be interpreted as an increase in structural integrity. These results did not change when including the control group, strongly confirming that these findings are not biased by any typical developmental changes. Moreover, they did not depend on the values assigned to the fixed effect of surgery in controls, confirming the stability of the results. This plasticity occurred after the closing of the putative sensitive period for visual development, at around 5 to 7 y of age (17).

What are the likely neural mechanisms underlying our results? Current dMRI methods are unable to determine the exact mechanism underlying the observed changes. Previous studies of structural plasticity have assessed changes in white matter structure over relatively short time courses, on the scale of days to months. White matter changes over these shorter time courses may reflect transient neural mechanisms such as the proliferation of oligodendrocytes and their precursor cells (57). Patients in the current study were tracked over a period of years, rather than days or months. It is therefore likely that the observed structural changes were stable and resulted from mechanisms such as myelin remodeling and bouton sprouting, rather than glial activity. To reduce the risk of false positives, we employed conservative FDR-based testing. However, this approach may have also introduced false negatives, such that potentially significant effects were lost.

Among the white matter pathways included in this study, we observed significant structural changes mainly in late-visual pathways. Age-related changes indicate an increase of structural integrity as a function of age, confirming previous findings of plasticity during adulthood in later areas (34, 35). Surgery-related changes indicate that part of the observed increase of structural integrity is predicted by time since surgery and not by maturational changes: It confirms that neural plasticity of late-visual pathways follows visual restoration even in adolescence. Interestingly, the effect of treatment on these tracts was influenced by the age at treatment: Patients who received interventions earlier rather than later in adolescence show greater increase of structural integrity.

What may be the function of the identified late-visual pathways in visual perception? Broadly speaking, these pathways can be classified as playing a role in visually guided behavior. The tasks of visual object and face recognition, visual memory, semantic processing, and linking object representation with lexical labels are thought to involve the ILF, which links extrastriate visual areas with temporal regions (58, 59). Another critical pathway that connects the fusiform gyrus with higher-level cortical regions (frontal) is the IFOF, that originates in the lingual and inferior occipital gyrus and terminates in the frontal lobe (60). Integration of somatosensory information, oculomotor coordination, voluntary orientation of attention, and motor planning are central tasks of the SLF (61, 62), an association fiber tract connecting both temporoparietal junction area and parietal lobe with the frontal lobe (63). Finally, the communication of sensory information between the two halves of the visual cortex is the main function of the posterior callosum forceps, an interhemispheric tract that

projects fibers from the splenium of the corpus callosum to connect homotopic occipital regions in the hemispheres. Moreover, we observed that structural changes in SLF, IFOF, and posterior callosum forceps are associated with behavioral improvement in face discrimination while controlling for age. These results indicate that late-visual pathways, that show already a surgery-related effect, influence behavioral performance: The increase in structural integrity (increase of FA and decrease of MD) correlates with the increase of behavioral performance in a face perception task. These results are not surprising as the IFOF has been shown to connect the fusiform gyrus with frontal regions (60), and the callosum tracts of the splenium connect homologous extrastriate areas of the two hemispheres relevant for higher-level visual tasks.

Age-related effects were observed in all non-visual pathways in terms of increase of FA or decrease of MD, while a surgery-related effect was observed only in the anterior callosum forceps when including the fixed effect of the group. This tract projects fibers from the genu of the corpus callosum to connect the medial and lateral surfaces of the frontal lobes. Increased structural integrity of the genu of the corpus callosum has been shown to correlate positively with working memory and problem-solving abilities in healthy young and elderly adults (64, 65), and an increase in FA has been linked to higher processing speed, more efficient verbal and nonverbal working memory, and enhanced cognitive flexibility (66). These results, together with the significant effect of treatment on the posterior callosum forceps, indicate that pathways connecting left and right homotopic visual areas are sensitive to visual restoration as their integrity significantly increased after surgery.

On the other hand, we did not observe any evidence of structural plasticity in early parts of the visual hierarchy in our study, in agreement with the classic conception that the critical window has already closed by the time of intervention (6). These findings are consistent with several studies in animal models of less severe perceptual disorders, such as amblyopia, that typically report a lack of change in early-visual pathways following intervention past the sensitive period (6, 67). The between-group difference confirms that structural integrity is reduced as a consequence of the visual deprivation and cannot reach normative values if visual restoration happens after the closure of the sensitive period.

Among all the tracts in which we found significant pairwise relations between treatment, structural changes, and behavioral improvement, we show that only changes in the posterior callosum forceps positively modulate the relationship between surgical intervention and behavioral improvement in face perception.

Limitations. It is important to mention some limitations of this study. First of all, despite the substantial number of patients in our clinical sample, it is important to notice that the collection of both behavioral and diffusion measurements could not be precisely time-triggered: Indeed, the number as well as the time window between diffusion data and behavioral measurements differs among patients, due to the challenging conditions of data collection.

Second, the inclusion of controls adds value to the study, as it allows us to assess the typical development of structural measures in healthy age-matched brains and to confirm that the surgery-related structural changes were not biased by age-related changes. Despite that, we should mention that the differences in the acquisition sequence of patients' and controls' data as well as the relevant differences in the clinical populations (rural Indian vs. US adolescents) require that we treat the interpretation of the fixed effect of group results with caution: We observed differences in multiple tracts (mainly in MD, see *SI Appendix*, Table S3 and S4), but these effects might have been due to differences in acquisition protocol, environmental and socioeconomic differences, or differences actually due to visual deprivation early in life. We compensated for some of the data acquisition differences by reducing the number of shells for data from controls, but other factors might still have impacted these results.

Conclusions. Our results show an improvement of behavioral performance following visual restoration mainly in a task assessing higher-level visual skills, as face perception, even after the closure of the sensitive period of development. This result is in agreement with the existence of an innate neural system that mediates the perception of faces at birth (68). Nevertheless, the difference with the latter study is significant: While Johnson et al. refer to a subcortical face-detection pathway, we refer to long-range late-visual pathways that predict behavioral improvement. In addition, our neuroimaging findings are in agreement with the idea that higher-order visual functions and extrastriate visual areas rely more on visual experience than basic visual functions and the primary visual cortex. Indeed, we observed a significant increase of surgery-related structural integrity in late-visual pathways mediating high-level visual functions (for a review see ref. 41). Unfortunately, in this study, we did not assess the functional activation corresponding to face perception in our sight recovery sample, so we cannot rule out the possibility that both activation and functional connectivity of the face recognition network are altered in these patients (69).

Besides arguing for a reconsideration of the timelines of cortical plasticity of long-range late-visual pathways, the observed sight-recovery-induced white matter changes in late-visual pathways advocate for the surgical treatment of visual disorders past the putative sensitive period for visual development. Such treatment can result in broad behavioral and neural gains, substantially improving the functional outlook and potential for these patients.

Methods

Participants. All work was carried out in accordance with the Code of Ethics of the World Medical Association (Declaration of Helsinki, 2008 (70)) and was approved by the Institutional Review Boards of Dr. Shroff's Charity Eye Hospital (Delhi, India) and the Massachusetts Institute of Technology (Cambridge, Massachusetts, United States). Informed consent was obtained from all participants, and all participants were evaluated and treated by licensed medical professionals at Dr. Shroff's Charity Hospital in Delhi, India.

Cataract Patients. Enrolled in this study were 23 cataract patients (6 female) aged 7 to 21 y (mean age of 12.34 ± 3.69 y at the time of surgery) (*SI Appendix*, Table S5). Patients were screened and recruited from the state of Uttar Pradesh, India, and received treatment under the purview of Project Prakash. They had been identified via the project's pediatric ophthalmic screening program in rural areas of India. All had dense bilateral cataracts since before 1 y of age and had received no prior eye care. Assessment of congeniality of deprivation was based on parental reports, ophthalmic examination of the eyeball (B-scans to assess for microphthalmos), consideration of cataract morphology (lamellar, polar, and total cataracts are indicative of congenital origins), and the presence of nystagmus, which is known to be induced by profound visual impairment very early in life (for a study on monkeys, see ref. 71). All patients received artificial intraocular lens implants, with additional correction provided by glasses and other low-vision aids. Consent was obtained separately for surgery and scientific studies.

Three patients (P13, P15, and P22) were excluded from subsequent analysis because all dMRI data acquisition occurred past 20 y of age. One patient (P18) was excluded as no behavioral measures were obtained. Patient ages were reported to the nearest year by parents or guardians. Because of limited record-keeping among rural families, exact birthdays were not available, and all analyses were based on the closest estimated age provided at the time of surgery. In addition to the sample of patients, we included 80 age-matched controls extracted from the 3T HCP-D (https://www.humanconnectome.org/study/hcp-lifespan-development) (42, 72) (mean age of 12.75 ± 3.3 y at the time of surgery).

Behavioral Methods. Patients participated in a number of behavioral tasks, including preoperative and postoperative longitudinal assessment of visual acuity and face discrimination. Nineteen patients had their visual acuity measured an average of 7.9 ± 3.9 times, and their performance on the facial discrimination test was assessed an average of 4.2 ± 2.0 times over the course of the study (150 total acuity timepoints and 79 total face discrimination timepoints). In the acuity task, patients were asked to identify stimuli of varying sizes at a viewing distance of 40 cm, with logMAR acuity estimates generated for each assessment. In the facial discrimination task, patients were asked to verbally discriminate between face stimuli (genuine face images) and nonface objects (NF0 in ref. 20) in a "yes–no" paradigm. Presentations were self-timed, so the stimulus disappeared when the patient provided a verbal response. The set comprised 300 stimuli, each one presented in a separate trial. D-prime scores were generated for each session considering responses to face as hits and to nonface as false alarms. Further methodological details for these tasks as well as performance results for a smaller cohort of patients are available in prior publications from our group (20).

For both behavioral tasks, we assessed the relative effects of time since surgery and age on performance using LMEs models. These models included fixed effects of age at the time of behavioral measurement and a logarithmic term for time since surgery as well as an interaction effect between age and log days since surgery (mean = 1.84; range = 0 to 3.42). The largest behavioral changes were noted in the period immediately following surgery, with smaller changes over time. To best fit this data, we tested models using both linear and logarithmic time since surgery terms. We selected the model with a logarithmic days since surgery term as it explained a larger proportion of variance, when compared to a model using a linear days since surgery term (as assessed by BIC). Visual inspection of the data (Fig. 1*B*) supports this log-linear relationship.

Using these models, we were able to assess the relative contributions of surgery (and subsequent restoration of visual input) and age-related maturational effects on visual performance. Additionally, by including an interaction term within the model, we were able to assess the extent to which age at intervention interacted with time since surgery, allowing for interrogation of potential windows of plasticity for these visual behavioral modalities.

MRI Data Acquisition. Brain imaging data of patients were obtained at the Mahajan Imaging Center, Defense Colony (New Delhi, India) using a GE Discovery MR750w 3T MRI scanner (GE Healthcare, Inc, Chicago, IL, USA) equipped with a 32-channel head coil. For each subject, a structural whole-brain T1-weighted anatomical scan (3.7 ms TE; 9.5 ms TR; 1 × 1 × 1 mm^3 isotropic voxels) was acquired. In the same session, a diffusion-weighted imaging sequence was performed with a 40-direction diffusion-weighted scan acquired in the anterior to posterior (AP) phase-encoding direction (74.4 ms TE; 13.73 s TR; 0.86 × 0.86 × 2 mm^3 anisotropic voxels; b = 1,000 s/mm^2; reconstruction matrix FOV: 220 × 220 × 144 mm, LR × AP × IS). Four dMRI sessions (one individual scan for four cataract patients) were inadvertently acquired with left to right (LR) phase encoding. Preprocessing steps for these data points were modified accordingly. This discrepancy in phase-encoding direction did not appear to meaningfully impact tractography results or data quality, so these data points were included in the analysis. Details of the HCP-D brain imaging acquisition protocol are extensively described in ref. 72.

Data Processing and Analysis. Preprocessing steps for the sample of patients were completed based on previously published methods (73) using the VistaSoft software package (Stanford University, Stanford, California) in addition to a more recent deep learning approach (73, 74). Data from the sample of controls were preprocessed by running the HCP Structural and Diffusion Preprocessing Pipelines, as part of the HCP Minimal Preprocessing pipeline (75).

In both samples, the visual pathways were derived through probabilistic tractography using MRtrix3 (Brain Institute, Melbourne, Australia) (76–85), while a whole-brain streamlines tracking (STT) tractography was used to extract late-visual and non-visual pathways. Diffusion properties (MD and FA) were sampled from the volumetric region defined by each white matter pathway extracted from the subject's longitudinal scan. Averaged MD and FA values were analyzed through LME models, to evaluate the longitudinal effects of maturation and cataract surgery on white matter development in patients. To correct for multiple-comparisons, we applied the Benjamini and Hochberg FDR test (86) separately for FA and MD values. Finally, we performed a mediation analysis using the MATLAB-based mediation toolbox described by Wager et al. (2008) (51); available at https://github.com/canlab/MediationToolbox) to assess the association between surgery, structural measures changes, and behavioral outcome.

Data, Materials, and Software Availability. Anonymized neuroimaging and behavioral data as well as analysis codes have been deposited in the Open Science Framework (https://osf.io/h7mb5/) (87).

ACKNOWLEDGMENTS. We thank Brian Allen for assistance with dMRI data processing and analysis. Funding and Support: C*ore Technology Platforms resources at New York University Abu Dhabi*. ASPIRE, the technology program management pillar of Abu Dhabi's Advanced Technology Research Council, via the ASPIRE Precision Medicine Research Institute Abu Dhabi (VRI-20-10). *High Performance Computing resources at New York University Abu Dhabi*. National Institute of Mental Health of the NIH Award Number U01MH109589. Project Prakash is supported by NIH NEI Grant No. R01EY020517, and grants from the Nick Simons Foundation, the Sikand Foundation, and the Halis Foundation. The content is solely the responsibility of the authors and does not necessarily represent the official views of the funding agencies.

Author affiliations: [a]Psychology, Division of Science, New York University, Abu Dhabi, United Arab Emirates; [b]University of Minnesota Medical School–Minneapolis, MN 55455; [c]Department of Electrical Engineering, Indian Institute of Technology, New Delhi, Delhi 110016, India; [d]Department of Brain and Cognitive Sciences, Massachusetts Institute of Technology, Cambridge, MA 02139; [e]Mahajan Imaging Center, Defence Colony, New Delhi, Delhi 110016, India; and [f]ASPIRE Precision Medicine Research Institute, Abu Dhabi, United Arab Emirates

1. S. Sheeladevi, J. G. Lawrenson, A. R. Fielder, C. M. Suttle, Global prevalence of childhood cataract: A systematic review. *Eye* **30**, 1160–1169 (2016).
2. S. R. Lambert *et al.*, Is there a latent period for the surgical treatment of children with dense bilateral congenital cataracts? *J. AAPOS* **10**, 30–36 (2006).
3. S. K. Dorairaj *et al.*, Childhood blindness in a rural population of southern India: Prevalence and etiology. *Ophthalmic Epidemiol.* **15**, 176–182 (2008).
4. B. S. Demissie, A. W. Solomon, Magnitude and causes of childhood blindness and severe visual impairment in Sekoru District, Southwest Ethiopia: A survey using the key informant method. *Trans. R. Soc. Trop. Med. Hyg.* **105**, 507–511 (2011).
5. M. Muhit *et al.*, The epidemiology of childhood blindness and severe visual impairment in Indonesia. *Br. J. Ophthalmol.* **102**, 1543–1549 (2018).
6. D. H. Hubel, T. N. Wiesel, The period of susceptibility to the physiological effects of unilateral eye closure in kittens. *J. Physiol.* **206**, 419–436 (1970).
7. B. Röder, P. Ley, B. H. Shenoy, R. Kekunnaya, D. Bottari, Sensitive periods for the functional specialization of the neural system for human face processing. *Proc. Natl. Acad. Sci. U.S.A.* **110**, 16760–16765 (2013).
8. P. Voss, Sensitive and critical periods in visual sensory deprivation. *Front. Psychol.* **4**, 664 (2013).
9. T. L. Lewis, D. Maurer, Multiple sensitive periods in human visual development: Evidence from visually deprived children. *Dev. Psychobiol.* **46**, 163–183 (2005).
10. B. Röder, R. Kekunnaya, M. J. S. Guerreiro, Neural mechanisms of visual sensitive periods in humans. *Neurosci. Biobehav. Rev.* **120**, 86–99 (2021).
11. P. Voss, F. Gougoux, R. J. Zatorre, M. Lassonde, F. Lepore, Differential occipital responses in early- and late-blind individuals during a sound-source discrimination task. *Neuroimage* **40**, 746–758 (2008).
12. P. Voss, F. Gougoux, M. Lassonde, R. J. Zatorre, F. Lepore, A positron emission tomography study during auditory localization by late-onset blind individuals. *NeuroReport* **17**, 383–388 (2006).
13. H. Burton, D. G. McLaren, Visual cortex activation in late-onset, Braille naive blind individuals: An fMRI study during semantic and phonological tasks with heard words. *Neurosci. Lett.* **392**, 38–42 (2006).
14. H. Burton *et al.*, Adaptive changes in early and late blind: A fMRI study of Braille reading. *J. Neurophysiol.* **87**, 589–607 (2002).
15. A. Pascual-Leone, A. Amedi, F. Fregni, L. B. Merabet, The plastic human brain cortex. *Annu. Rev. Neurosci.* **28**, 377–401 (2005).
16. M. Bedny, Evidence from blindness for a cognitively pluripotent cortex. *Trends Cogn. Sci.* **21**, 637–648 (2017).
17. D. Maurer, T. L. Lewis, "Sensitive periods in visual development" in *The Oxford Handbook of Developmental Psychology*, P. D. Zelazo, Ed. (Oxford Academic, 2013), **vol. 1**, pp. 202–235.
18. S. Ganesh *et al.*, Results of late surgical intervention in children with early-onset bilateral cataracts. *Br. J. Ophthalmol.* **98**, 1424–1428 (2014).
19. A. Kalia *et al.*, Development of pattern vision following early and extended blindness. *Proc. Natl. Acad. Sci. U.S.A.* **111**, 2035–2039 (2014).
20. T. K. Gandhi, A. K. Singh, P. Swami, S. Ganesh, P. Sinha, Emergence of categorical face perception after extended early-onset blindness. *Proc. Natl. Acad. Sci. U.S.A.* **114**, 6139–6143 (2017).

21. M. S. Hussen, K. L. Gebreselassie, M. A. Seid, G. T. Belete, Visual outcome of cataract surgery at Gondar University Hospital Tertiary Eye Care and Training Center, North West Ethiopia. *Clin. Optom. (Auckl)* **9**, 19–23 (2017).
22. A. M. Beyene, A. Eshetie, Y. Tadesse, M. G. Getnet, Time to recovery from cataract and its predictors among eye cataract patients treated with cataract surgery: A retrospective cohort study in Ethiopia. *Ann. Med. Surg. (Lond)* **65**, 102275 (2021).
23. D. Sagi, Perceptual learning in vision research. *Vision Res.* **51**, 1552–1566 (2011).
24. Q. He, S. Gan, Neural mechanisms of visual field recovery after perceptual training in cortical blindness. *J. Neurosci.* **42**, 1886–1887 (2022).
25. A. Barbot *et al.*, Spared perilesional V1 activity underlies training-induced recovery of luminance detection sensitivity in cortically-blind patients. *Nat. Commun.* **12**, 6102 (2021).
26. S. Ajina, C. Kennard, G. Rees, H. Bridge, Motion area V5/MT+ response to global motion in the absence of V1 resembles early visual cortex. *Brain* **138**, 164–178 (2015).
27. C. Y. L. Huh *et al.*, Retinoid therapy restores eye-specific cortical responses in adult mice with retinal degeneration. *Curr. Biol.* **32**, 4538–4546.e5 (2022).
28. D. Bottari *et al.*, The neural development of the biological motion processing system does not rely on early visual input. *Cortex* **71**, 359–367 (2015).
29. E. Castaldi, C. Lunghi, M. C. Morrone, Neuroplasticity in adult human visual cortex. *Neurosci. Biobehav. Rev.* **112**, 542–552 (2020).
30. D. Bottari *et al.*, Sight restoration after congenital blindness does not reinstate alpha oscillatory activity in humans. *Sci. Rep.* **6**, 24683 (2016).
31. J. M. Holmes, M. P. Clarke, Amblyopia. *Lancet* **367**, 1343–1351 (2006).
32. D. M. Levi, D. C. Knill, D. Bavelier, Stereopsis and amblyopia: A mini-review. *Vision Res.* **114**, 17–30 (2015).
33. B. Thompson, M. Y. Villeneuve, C. Casanova, R. F. Hess, Abnormal cortical processing of pattern motion in amblyopia: Evidence from fMRI. *Neuroimage* **60**, 1307–1315 (2012).
34. B. Draganski *et al.*, Changes in grey matter induced by training. *Nature* **427**, 311–312 (2004).
35. I. Gauthier, M. J. Tarr, A. W. Anderson, P. Skudlarski, J. C. Gore, Activation of the middle fusiform'face area'increases with expertise in recognizing novel objects. *Nat. Neurosci.* **2**, 568–573 (1999).
36. J. Hyvärinen, S. Carlson, L. Hyvärinen, Early visual deprivation alters modality of neuronal responses in area 19 of monkey cortex. *Neurosci. Lett.* **26**, 239–243 (1981).
37. S. Sourav, D. Bottari, R. Kekunnaya, B. Röder, Evidence of a retinotopic organization of early visual cortex but impaired extrastriate processing in sight recovery individuals. *J. Vis.* **18**, 22 (2018).
38. E. Striem-Amit *et al.*, Functional connectivity of visual cortex in the blind follows retinotopic organization principles. *Brain* **138**, 1679–1695 (2015).
39. K. Pitchaimuthu *et al.*, Steady state evoked potentials indicate changes in nonlinear neural mechanisms of vision in sight recovery individuals. *Cortex* **144**, 15–28 (2021).
40. T. L. Lewis, D. Maurer, Effects of early pattern deprivation on visual development. *Optom. Vis. Sci.* **86**, 640–646 (2009).
41. B. Röder, R. Kekunnaya, Visual experience dependent plasticity in humans. *Curr. Opin. Neurobiol.* **67**, 155–162 (2021).
42. L. H. Somerville *et al.*, The lifespan human connectome project in development: A large-scale study of brain connectivity development in 5–21 year olds. *Neuroimage* **183**, 456–468 (2018).
43. A. Kalia *et al.*, Assessing the impact of a program for late surgical intervention in early-blind children. *Publ. Health* **146**, 15–23 (2017).
44. N. Barnea-Goraly *et al.*, White matter development during childhood and adolescence: A cross-sectional diffusion tensor imaging study. *Cereb. Cortex* **15**, 1848–1854 (2005).
45. C. Lebel *et al.*, Diffusion tensor imaging of white matter tract evolution over the lifespan. *Neuroimage* **60**, 340–352 (2012).
46. D. Qiu, L.-H. Tan, K. Zhou, P.-L. Khong, Diffusion tensor imaging of normal white matter maturation from late childhood to young adulthood: Voxel-wise evaluation of mean diffusivity, fractional anisotropy, radial and axial diffusivities, and correlation with reading development. *Neuroimage* **41**, 223–232 (2008).
47. V. J. Schmithorst, M. Wilke, B. J. Dardzinski, S. K. Holland, Correlation of white matter diffusivity and anisotropy with age during childhood and adolescence: A cross-sectional diffusion-tensor MR imaging study. *Radiology* **222**, 212–218 (2002).
48. D. Maurer, C. J. Mondloch, T. L. Lewis, Sleeper effects. *Dev. Sci.* **10**, 40–47 (2007).
49. V. J. Schmithorst, W. Yuan, White matter development during adolescence as shown by diffusion MRI. *Brain Cogn.* **72**, 16–25 (2010).
50. C. K. Tamnes, D. R. Roalf, A.-L. Goddings, C. Lebel, Diffusion MRI of white matter microstructure development in childhood and adolescence: Methods, challenges and progress. *Dev. Cogn. Neurosci.* **33**, 161–175 (2018).
51. T. D. Wager, M. L. Davidson, B. L. Hughes, M. A. Lindquist, K. N. Ochsner, Prefrontal-subcortical pathways mediating successful emotion regulation. *Neuron* **59**, 1037–1050 (2008).
52. R. M. Baron, D. A. Kenny, The moderator–mediator variable distinction in social psychological research: Conceptual, strategic, and statistical considerations. *J. Pers. Soc. Psychol.* **51**, 1173–1182 (1986).
53. T. L. Lewis, D. Maurer, H. P. Brent, Development of grating acuity in children treated for unilateral or bilateral congenital cataract. *Invest. Ophthalmol. Vis. Sci.* **36**, 2080–2095 (1995).
54. T. K. Gandhi, S. Ganesh, P. Sinha, Improvement in spatial imagery following sight onset late in childhood. *Psychol. Sci.* **25**, 693–701 (2014).
55. C. J. Mondloch *et al.*, The effect of early visual deprivation on the development of face detection. *Dev. Sci.* **16**, 728–742 (2013).
56. T. Paus, Growth of white matter in the adolescent brain: Myelin or axon? *Brain Cogn.* **72**, 26–35 (2010).
57. R. D. Fields, A new mechanism of nervous system plasticity: Activity-dependent myelination. *Nat. Rev. Neurosci.* **16**, 756–767 (2015).
58. M. Catani, D. K. Jones, R. Donato, D. H. Ffytche, Occipito-temporal connections in the human brain. *Brain* **126**, 2093–2107 (2003).
59. C. J. Mummery *et al.*, Disrupted temporal lobe connections in semantic dementia. *Brain* **122**, 61–73 (1999).
60. A. H. Palejwala *et al.*, Anatomy and white matter connections of the fusiform gyrus. *Sci. Rep.* **10**, 13489 (2020).
61. X. Wang *et al.*, Subcomponents and connectivity of the superior longitudinal fasciculus in the human brain. *Brain Struct. Funct.* **221**, 2075–2092 (2016).
62. M. Corbetta, G. L. Shulman, Control of goal-directed and stimulus-driven attention in the brain. *Nat. Rev. Neurosci.* **3**, 201–215 (2002).
63. N. Makris *et al.*, Segmentation of subcomponents within the superior longitudinal fascicle in humans: A quantitative, in vivo, DT-MRI study. *Cereb. Cortex* **15**, 854–869 (2005).
64. N. M. Zahr, T. Rohlfing, A. Pfefferbaum, E. V. Sullivan, Problem solving, working memory, and motor correlates of association and commissural fiber bundles in normal aging: A quantitative fiber tracking study. *Neuroimage* **44**, 1050–1062 (2009).
65. R. A. Charlton, T. R. Barrick, I. N. C. Lawes, H. S. Markus, R. G. Morris, White matter pathways associated with working memory in normal aging. *Cortex* **46**, 474–489 (2010).
66. K. M. Kennedy, N. Raz, Aging white matter and cognition: Differential effects of regional variations in diffusion properties on memory, executive functions, and speed. *Neuropsychologia* **47**, 916–927 (2009).
67. N. Daw, *Visual Development* (Springer, US, 2013).
68. M. H. Johnson, Subcortical face processing. *Nat. Rev. Neurosci.* **6**, 766–774 (2005).
69. C. L. Grady, C. J. Mondloch, T. L. Lewis, D. Maurer, Early visual deprivation from congenital cataracts disrupts activity and functional connectivity in the face network. *Neuropsychologia* **57**, 122–139 (2014).
70. World Medical Association. Declaration of Helsinki, *Ethical Principles for Medical Research Involving Human Subjects* (2008).
71. R. J. Tusa, M. X. Repka, C. B. Smith, S. J. Herdman, Early visual deprivation results in persistent strabismus and nystagmus in monkeys. *Invest. Ophthalmol. Vis. Sci.* **32**, 134–141 (1991).
72. M. P. Harms *et al.*, Extending the human connectome project across ages: Imaging protocols for the lifespan development and aging projects. *Neuroimage* **183**, 972–984 (2018).
73. K. G. Schilling *et al.*, Synthesized b0 for diffusion distortion correction (Synb0-DisCo). *Magn. Reson. Imaging* **64**, 62–70 (2019).
74. K. G. Schilling *et al.*, Distortion correction of diffusion weighted MRI without reverse phase-encoding scans or field-maps. *PLoS One* **15**, e0236418 (2020).
75. M. F. Glasser *et al.*, The minimal preprocessing pipelines for the human connectome project. *Neuroimage* **80**, 105–124 (2013).
76. P. J. Basser, D. K. Jones, Diffusion-tensor MRI: Theory, experimental design and data analysis–A technical review. *NMR Biomed.* **15**, 456–467 (2002).
77. T. E. J. Behrens *et al.*, Characterization and propagation of uncertainty in diffusion-weighted MR imaging. *Magn. Reson. Med.* **50**, 1077–1088 (2003).
78. F. Calamante, J.-D. Tournier, G. D. Jackson, A. Connelly, Track-density imaging (TDI): Super-resolution white matter imaging using whole-brain track-density mapping. *Neuroimage* **53**, 1233–1243 (2010).
79. T. E. Conturo *et al.*, Tracking neuronal fiber pathways in the living human brain. *Proc. Natl. Acad. Sci. U.S.A.* **96**, 10422–10427 (1999).
80. S. Mori, P. C. M. van Zijl, Fiber tracking: Principles and strategies–A technical review. *NMR Biomed.* **15**, 468–480 (2002).
81. G. J. M. Parker, H. A. Haroon, C. A. M. Wheeler-Kingshott, A framework for a streamline-based probabilistic index of connectivity (PICo) using a structural interpretation of MRI diffusion measurements. *J. Magn. Reson. Imaging* **18**, 242–254 (2003).
82. J.-D. Tournier, F. Calamante, A. Connelly, Robust determination of the fibre orientation distribution in diffusion MRI: Non-negativity constrained super-resolved spherical deconvolution. *Neuroimage* **35**, 1459–1472 (2007).
83. J.-D. Tournier, F. Calamante, D. G. Gadian, A. Connelly, Direct estimation of the fiber orientation density function from diffusion-weighted MRI data using spherical deconvolution. *Neuroimage* **23**, 1176–1185 (2004).
84. J.-D. Tournier, F. Calamante, A. Connelly, MRtrix: Diffusion tractography in crossing fiber regions. *Int. J. Imaging Syst. Technol.* **22**, 53–66 (2012).
85. J.-D. Tournier *et al.*, MRtrix3: A fast, flexible and open software framework for medical image processing and visualisation. *Neuroimage* **202**, 116137 (2019).
86. Y. Benjamini, Y. Hochberg, Controlling the false discovery rate: A practical and powerful approach to multiple testing. *J. R. Stat. Soc.* **57**, 289–300 (1995).
87. C. A. Pedersini *et al.*, White matter plasticity following cataract *surgery* in congenitally blind patients. Open Science *Framework*. https://osf.io/h7mb5/. Deposited 9 March 2023.